RESEARCH ARTICLE

Figures and figure supplements

Identification of functionally distinct macrophage subpopulations in *Drosophila*

Jonathon Alexis Coates *et al*

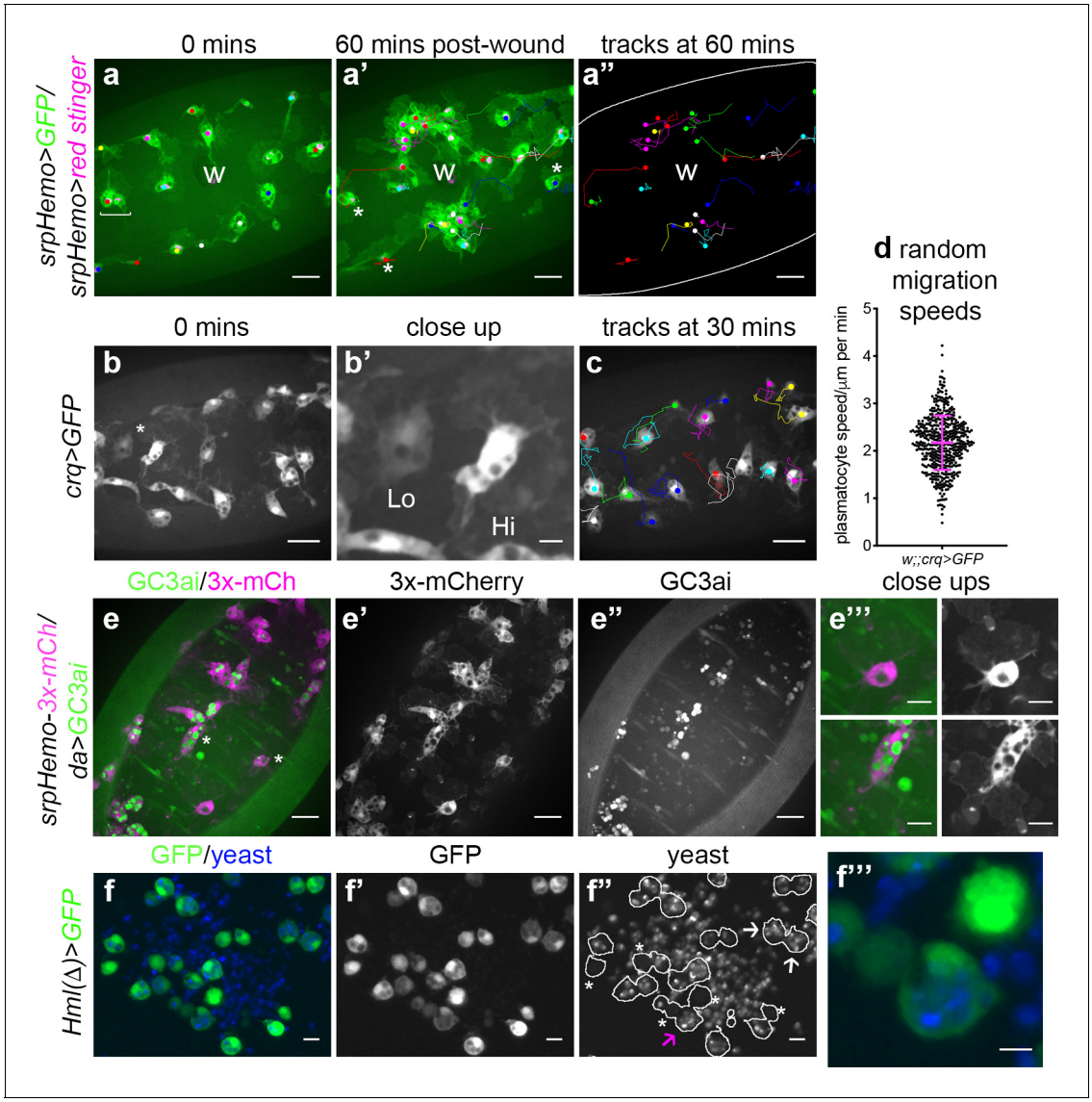

Figure 1. Heterogeneity of *Drosophila* embryonic plasmatocyte responses. (**a**) GFP (green) and nuclear red stinger (magenta) labelled plasmatocytes on the ventral side of a stage 15 embryo at 0 min (**a**) and 60 min post-wounding (**a'**); plasmatocyte tracks at each timepoint are overlaid (**a–a'**) or shown in full (**a''**). Examples of plasmatocytes failing to respond to the wound (w) indicated via asterisks; square bracket (**a**) indicates neighbouring plasmatocytes, one of which responds to wounding, while the other fails to respond (see ***Video 1***). (**b**) Imaging of plasmatocytes labelled using *crq-GAL4* to drive expression of GFP reveals a wide range in levels of *crq* promoter activity within plasmatocytes at stage 15; (**b'**) Close-up of cells marked by an asterisk in (**b**). (**c**) Overlay of plasmatocyte tracks of cells shown in (**b**) showing significant variation in their random migration speeds. (**d**) Scatterplot of plasmatocyte random migration speeds (taken from 23 embryos); line and error bars show mean and standard deviation, respectively. (**e**) Imaging the ventral midline at stage 15 shows a wide range in the amount of apoptotic cell clearance (green in merge; labelled via the caspase-sensitive reporter GC3ai) undertaken by plasmatocytes (magenta in merge, labelled via *srpHemo-3x-mCherry* reporter); (**e'–e''**) mCherry and GC3ai channels; (**e'''**) close-ups of cells devoid/full of engulfed GC3ai particles (indicated by asterisks in (**e**)). (**f**) Larval hemocytes (green in merge, labelled via *Hml(Δ)-GAL4*-driven expression of GFP) exhibit a range in their capacities to engulf calcofluor-labelled yeast (blue in merge) in vitro; (**f'–f''**) GFP and yeast channels; white lines indicate cell edges in (**f''**); asterisks in (**f''**) indicate cells that have failed to phagocytose yeast; white arrows in (**f''**) indicate cells that have phagocytosed multiple yeast particles; magenta arrow in (**f''**) indicates close-up of region indicated in (**f'''**). Scale bars represent 20 μm (**a–a'', b, c, e–e''**), 10 μm (**e''', f–f''**), or 5 μm (**b', f'''**). See ***Supplementary file 1*** for full list of genotypes.

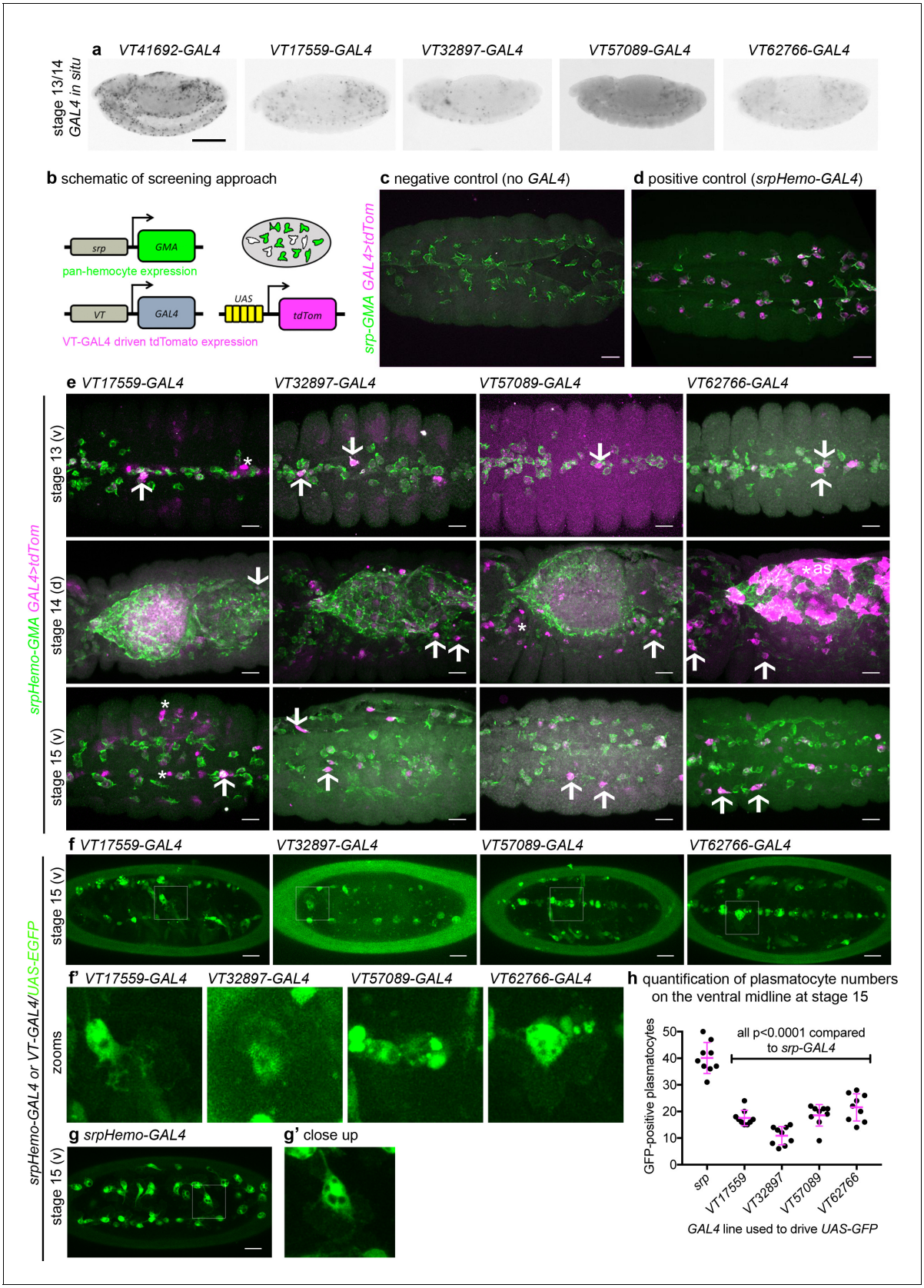

Figure 2. Identification of enhancers labelling discrete plasmatocyte subpopulations in *Drosophila*. (**a**) Lateral views of stage 13/14 embryos with in situ hybridisation performed for GAL4 for indicated *VT-GAL4* lines (anterior is left). Taken with permission from http://enhancers.starklab.org/ (n.b. these

Figure 2 continued on next page

Figure 2 continued

images are not covered by the CC-BY 4.0 licence and further reproduction of this panel would need permission from the copyright holder); *VT41692-GAL4* represents an example in which the majority of plasmatocytes are labelled. (**b**) Schematic diagram showing screening approach to identify subpopulations of plasmatocytes: *VT-GAL4*-positive plasmatocytes will express both GMA (green) and tdTomato (magenta) – white cells in the schematic. (**c–d**) Images showing the ventral midline at stage 14 of negative control (no driver; *w;UAS-tdTom/+;srpHemo-GMA*) and positive control (w; *srpHemo-GAL4/UAS-tdTom;srpHemo-GMA*) embryos. (**e**) Images showing embryos containing *VT-GAL4*-labelled cells (via *UAS-tdTomato*, shown in magenta) at stage 13 (first row, ventral views), stage 14 (second row, dorsal views), and stage 15 (third row, ventral views). The entire hemocyte population is labelled via *srpHemo-GMA* (green); arrows indicate examples of *VT-GAL4*-positive plasmatocytes; asterisks indicate *VT-GAL4*-positive cells that are not labelled by *srpHemo-GMA*. N.b. *VT62766-GAL4* image contrast enhanced to different parameters compared to other images owing to the very bright labelling of amnioserosal cells (cells on dorsal side of embryo destined to be removed during dorsal closure; labelled with an asterisk) in the stage 14 image. (**f**) Labelling of smaller numbers of plasmatocytes on the ventral midline at stage 15 using *VT-GAL4* lines indicated and *UAS-GFP* (green); boxed regions show close-ups of *VT-GAL4*-positive plasmatocytes (**f'**). (**g**) Ventral view of positive control embryo (*w;srpHemo-GAL4,UAS-GFP*) and example plasmatocyte (**g'**) at stage 15. (**h**) Scatterplot showing numbers plasmatocytes labelled using *VT-GAL4* lines to drive expression from *UAS-GFP* on the ventral midline at stage 15; lines and error bars represent mean and standard deviation, respectively. p-Values calculated via one-way ANOVA with a Dunnett's multiple comparison post-test (all compared to *srpHemo-GAL4* control); n = 9 embryos per genotype. Scale bars represent 150 μm (**a**) or 10 μm (**c–g**). See ***Supplementary file 1*** for full list of genotypes; overlap of VT enhancer expression with known plasmatocyte markers can be found in ***Figure 2—figure supplements 1*** and ***2***.

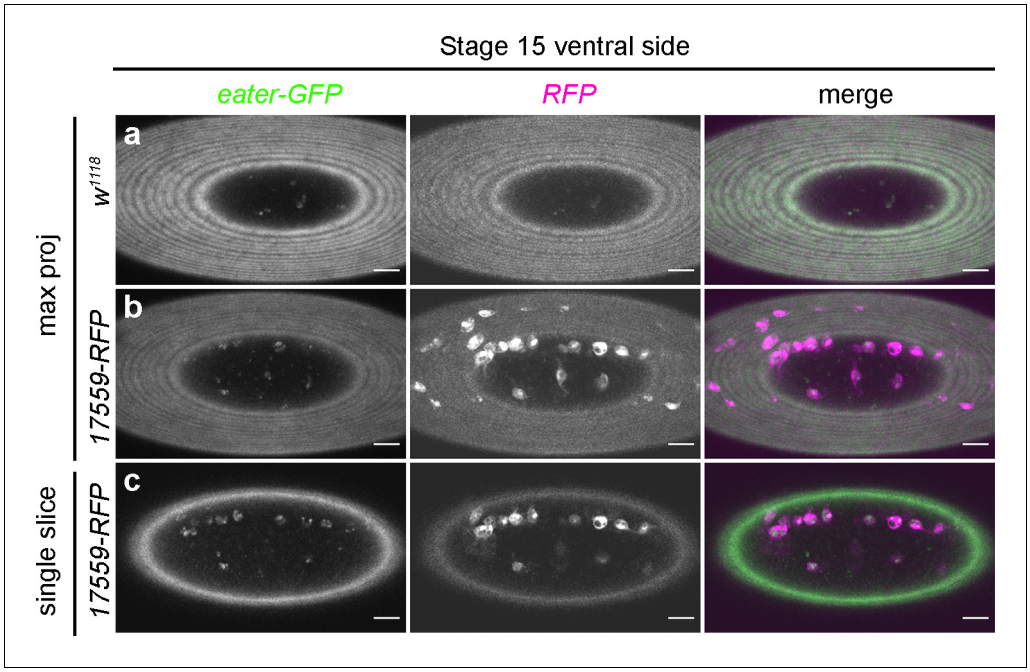

Figure 2—figure supplement 1. Subpopulation cells do not express *eater* in the embryo. (**a–b**) Maximum projections of the ventral surface of a negative control embryo (**a**) and an embryo containing *eater-GFP* and *VT17559-RFP* (**b**). Left-hand panels show GFP channel (green in merge); central panels show RFP channel (magenta in merge); right-hand panels show merged images. (**c**) Single z-slice taken from the z-series used to construct projection shown in (**b**) in order to confirm lack of *eater* expression in subpopulation cells. Scale bars represent 20 μm. See ***Supplementary file 1*** for full list of genotypes.

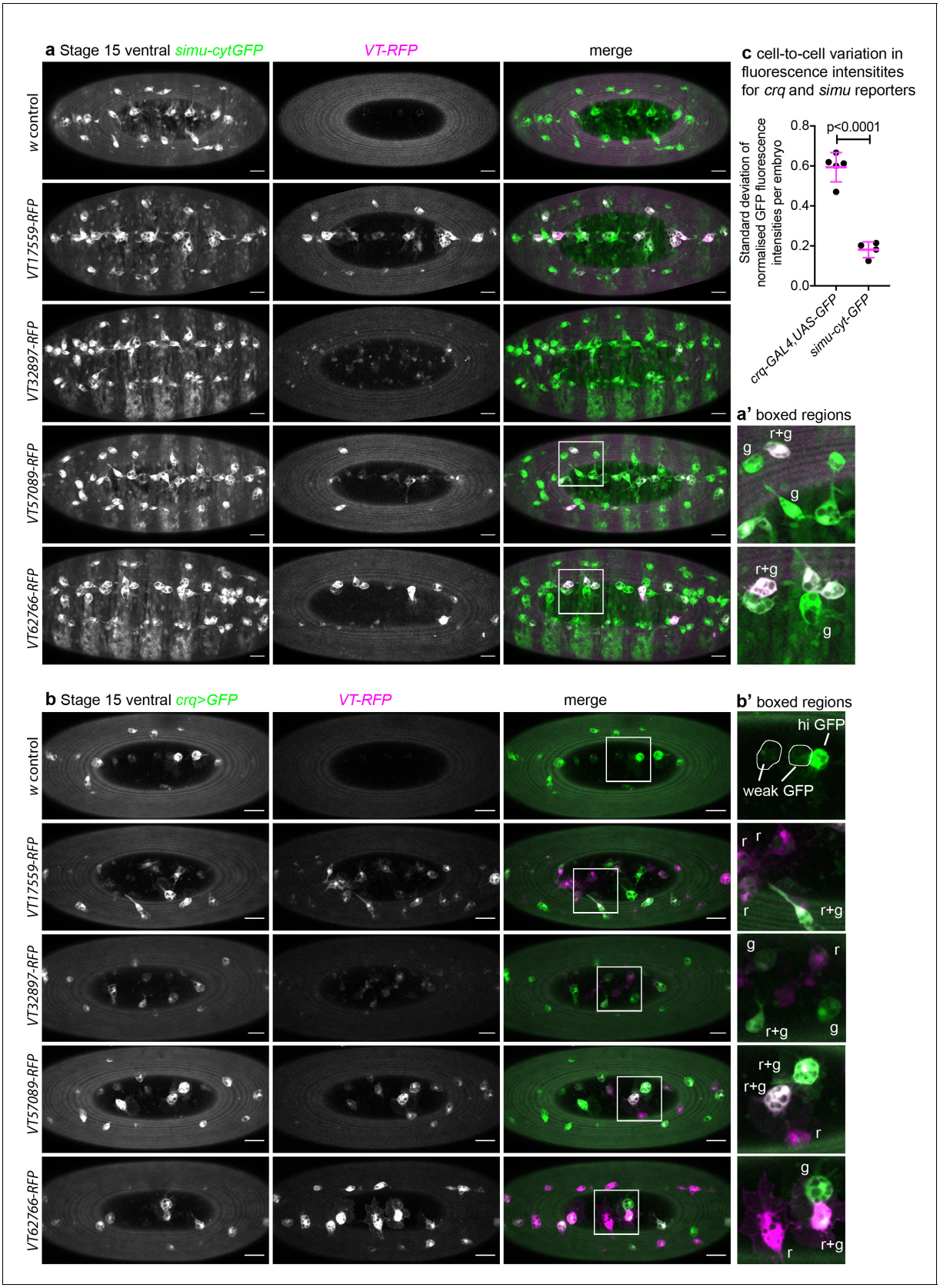

Figure 2—figure supplement 2. *crq* and *simu* do not specifically mark subpopulation cells in the developing embryo. (**a–b**) Maximum projections of the ventral surface of embryos containing *VT-RFP* and either *simu-cytGFP* (**a**) or *crq-GAL4,UAS-GFP* (**b**). Left-hand panels show *simu-cytGFP* (**a**, green in

Figure 2—figure supplement 2 continued on next page

Figure 2—figure supplement 2 continued

merge) or *crq-GAL4,UAS-GFP* (**b**, green in merge); central panels show RFP channel (magenta in merge); right-hand panels show merged images. (**a'–b'**) show enlarged regions indicated by white boxes in merged images; 'r', 'g', and 'r+g' denote cells expressing RFP only, GFP only or both fluorophores, respectively; w^{1118} embryos without a *VT-RFP* transgene used as negative control; scale bars denote 20 μm. (**c**) Scatterplot of the standard deviation of normalised GFP fluorescence intensity per plasmatocyte, per embryo in controls containing *crq-GAL4,UAS-GFP* or *simu-cytGFP*. Lines and error bars show mean and standard deviation, respectively; n = 5 and 4 embryos for *simu-cytGFP* and *crq-GAL4,UAS-GFP*, respectively; $p<0.0001$ via Student's t-test. See ***Supplementary file 1*** for full list of genotypes.

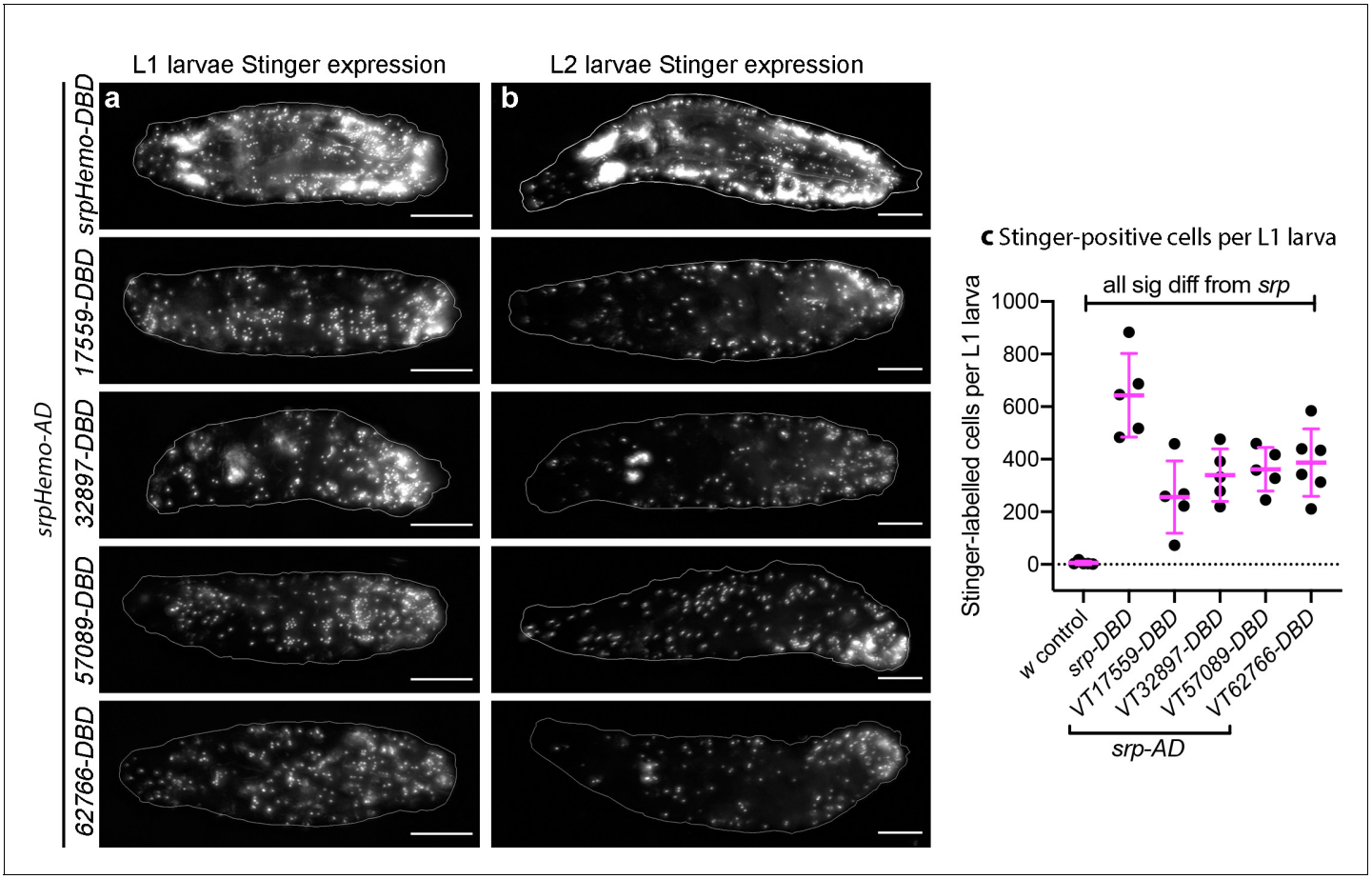

Figure 3. Plasmatocyte subpopulations are present in large numbers in L1 and L2 larvae. (**a–b**) Images of L1 (**a**) and L2 larvae (**b**) with cells labelled using the split GAL4 system (*srpHemo-AD* in combination with *srpHemo-DBD* or the *VT-DBD* transgene indicated) to drive expression from *UAS-stinger*. Scale bars represent 150 μm; white lines show edge of the larva; images contrast enhanced to 0.3% saturation. (**c**) Scatterplot showing numbers of Stinger-positive cells labelled via the split GAL4 system per larva; numbers of cells were quantified from flattened L1 larvae. w^{1118}*;UAS-stinger/+* larvae were used as negative controls; all conditions are significantly different compared to the positive control (w^{1118}*;srpHemo-AD/UAS-stinger; srpHemo-DBD/+*) via a one-way ANOVA with a Dunnett's multiple comparison post-test: *srp* vs *w*, p<0.0001; *srp* vs *VT17559* p<0.0001; *srp* vs VT32897, p=0.0013; *srp* vs *VT57089*, p=0.0029; *srp* vs *VT62766*, p=0.0047; n = 5 for *w* control, *srp*, *VT17559*, *VT32897*, and *VT57089* and n = 6 for *VT62766*. See ***Supplementary file 1*** for full list of genotypes; a schematic and validation of this split GAL4 approach in the embryo can be found in ***Figure 3—figure supplement 1***.

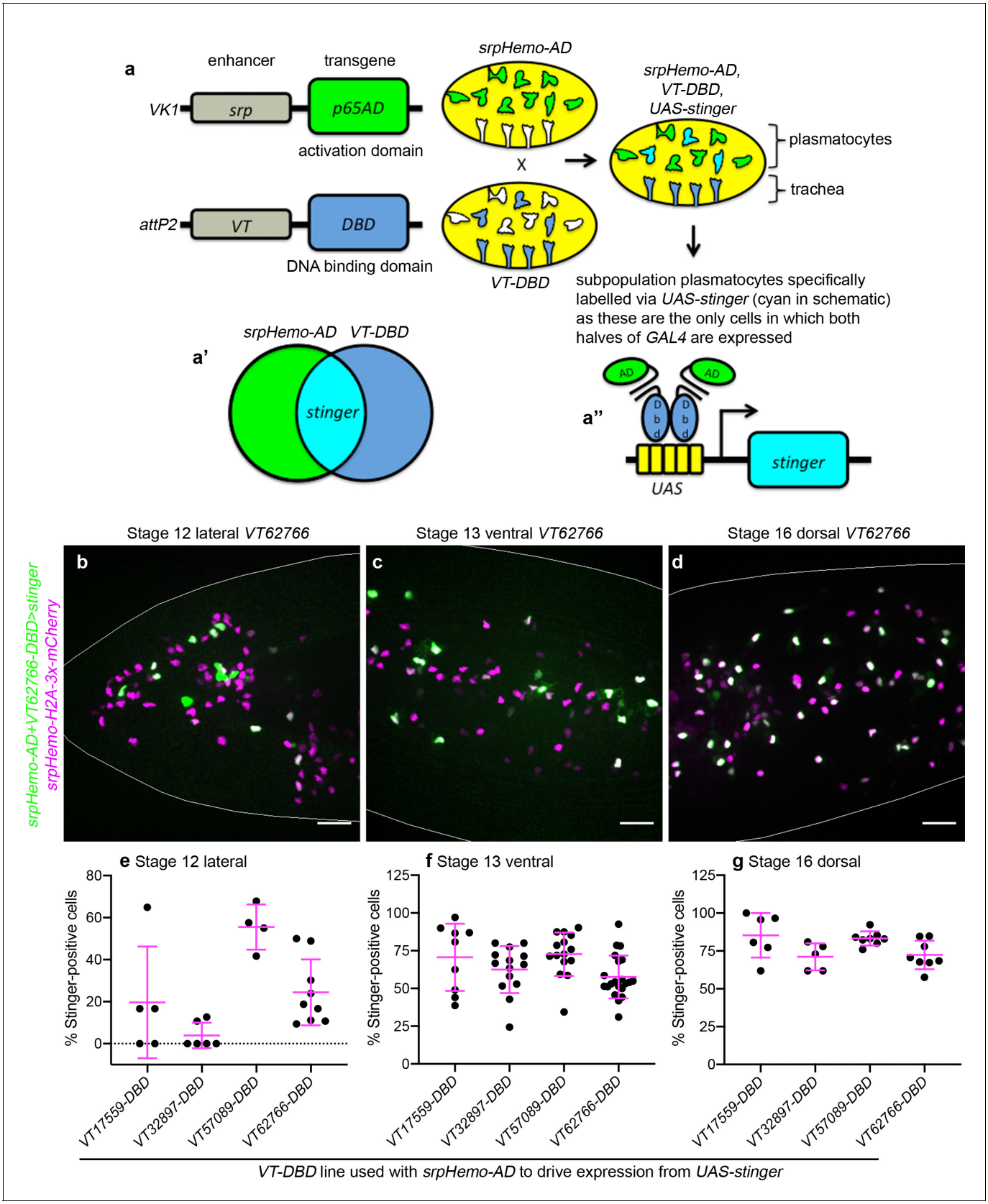

Figure 3—figure supplement 1. Using a split GAL4 approach to label plasmatocyte subpopulations. (**a**) *SrpHemo-AD* and *VT-DBD* transgenic flies were generated: *srpHemo-AD* drives expression of the activation domain (AD) of *GAL4* in all hemocytes (green), while VT enhancers drive expression of

Figure 3—figure supplement 1 continued on next page

Figure 3—figure supplement 1 continued

the DNA-binding domain (DBD) of *GAL4* in a subpopulation of plasmatocytes and, in the case of some VT enhancers, other cell types (dark blue). (**a'–a''**) Intersection of these expression patterns leads to the presence of both halves of *GAL4* (cyan) solely within those cells in which both *srp* and VT enhancer regions are active (**a''**). This approach restricts activation of transgenes under *UAS* control (e.g. *UAS-stinger*) to those cells that are double-positive for both *srp* and VT enhancer expression, ensuring expression is more specific to plasmatocyte subpopulations. (**b–d**) Maximum projections of live embryos containing *srpHemo-H2A-3x-mCherry* (all hemocytes, purple) and *UAS-Stinger* (green) driven via the split GAL4 system (*srpHemo-AD* in combination with the appropriate *VT-DBD*) at stages and orientations indicated. White lines show edges of the embryo; overlap of nuclear markers appears white; scale bars represent 20 μm. (**e–g**) Scattergraphs showing quantification of percentage of *srpHemo-H2A-3x-mCherry*-positive cells that are positive for Stinger expression in lateral regions of the head at stage 12 (**e**), on the ventral midline at stage 13 (**f**) and on the dorsal side of the embryo at stage 16 (**g**). See ***Supplementary file 1*** for full list of genotypes.

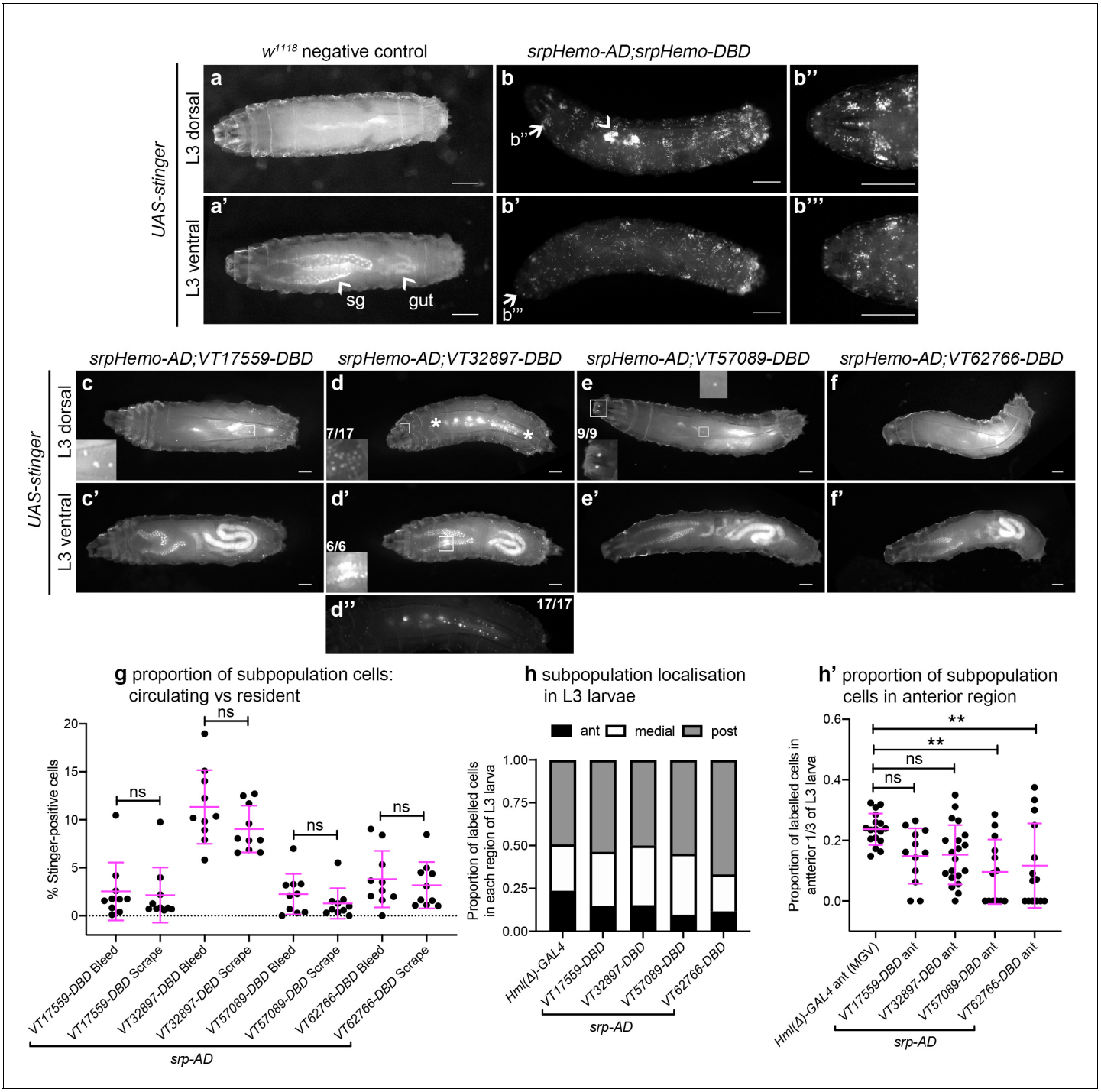

Figure 4. Plasmatocyte subpopulations are greatly reduced in L3 larvae but exhibit distinctive localisations. (**a–f**) Dorsal and ventral views of negative control L3 larvae (**a**, no GAL4), positive control L3 larvae with hemocytes labelled via *serpent* (**b**, *UAS-stinger* driven by *srpHemo-AD;srpHemo-DBD*) and L3 larvae containing cells labelled through expression of *UAS-stinger* via *srpHemo-AD* and the *VT-DBD* transgenes indicated (**c–f**). Arrowheads indicate non-specific expression of Stinger in salivary glands and gut (**a'** – also visible in dorsal images (**c'–f'**) but not labelled) and possible proventricular region hemocytes/garland cells (**b**); arrows (**b, b'**) indicate regions shown in close-ups of potential hemocyte population in the head region (**b''**) and in the Bolwig organ (**b'''**); boxes indicate individual hemocytes (**c, e**) and labelling in the head region (**d**), proventriculus/of Garland cells (**d'**), and Bolwig organ (**e**) shown at enhanced magnification in inset panels; asterisks in (**d**) denote region shown as a close-up and at a reduced brightness in (**d''**) in order to reveal detail of cells along the dorsal vessel; fractions indicate the number of larvae exhibiting a particular localisation out of the total imaged. (**g**) Scatterplot showing the proportion of subpopulation cells labelled via the split GAL4 system in circulation (initial bleed) compared to the proportions in resident/adhered populations (scraping of the carcass) in the indicated genotypes. Proportions obtained via each method compared via Student's t-test

Figure 4 continued on next page

Figure 4 continued

(n = 10 larvae per genotype; p=0.77 (*VT17559*), p=0.13 (*VT32897*), p=0.27 (*VT57089*), p=0.60 (*VT62766*)). (**h**) Bar chart showing the relative proportions of labelled cells found within the anterior, medial or posterior 1/3 of L3 larvae using *Hml(Δ)-GAL4* to drive EGFP or the split GAL4 system to express Stinger in all larval hemocytes or subpopulations, respectively (n = 17, 12, 20, 13, 14 larvae). (**h'**) Scatterplot of the proportions of cells found within the anterior region of L3 larvae for controls and split GAL4 lines. Kruskall-Wallis test with Dunn's multiple comparisons test was used to compare subpopulation values with *Hml(Δ)-GAL4* control; (p=0.11 (*VT17559*), p=0.061 (*VT32897*), p=0.0018 (*VT57089*), p=0.0063 (*VT62766*)). Scale bars represent 500 μm (**a–f**); larval images contrast enhanced to 0.3% saturation (**a–f**); lines and error bars represent mean and standard deviation, respectively (**g, h'**); bars represent mean (**h**); ns and ** denote not significant and p<0.01, respectively. See ***Supplementary file 1*** for full list of genotypes; see ***Figure 4—figure supplement 1*** for quantification of numbers of subpopulation cells labelled using the original *VT-GAL4* lines and lineage tracing of subpopulation cells via G-TRACE.

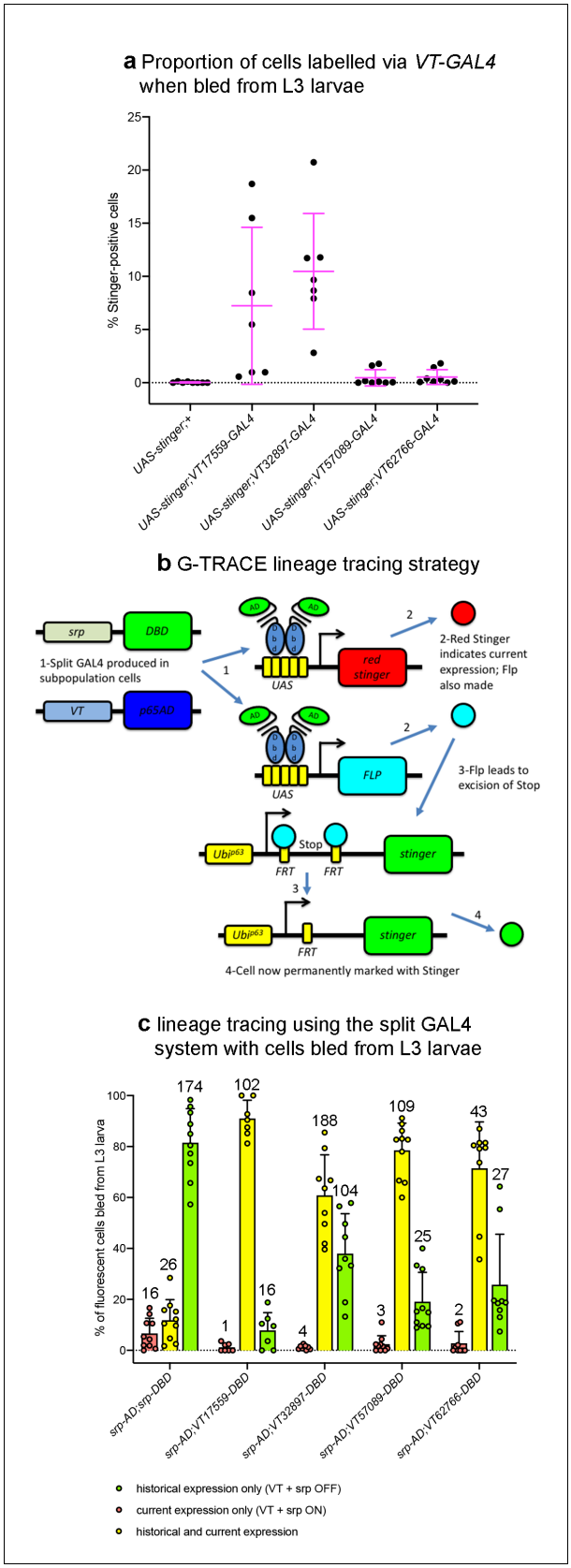

Figure 4—figure supplement 1. Lineage tracing shows reprogramming of subpopulation cells in L3 larvae. (**a**) Scatterplot showing proportion of cells that can be labelled via *VT-GAL4* (using *UAS-stinger* as a reporter) when

Figure 4—figure supplement 1 continued on next page

Figure 4—figure supplement 1 continued

bled from L3 larvae (i.e. labelled independently of a requirement for *serpent* expression); larvae containing *UAS-stinger,* but without a driver were used as a negative control. Each point represents a dissected larva (n = 8, 7, 7, 8 and 8, from left to right for indicated genotypes). Lines and error bars represent mean and standard deviation, respectively; genotypes were as follows: *w;UAS-stinger*, *w;UAS-stinger;VT-GAL4*. (**b**) Schematic use of G-TRACE system to lineage trace subpopulations in concert with split GAL4 transgenics. (**c**) Grouped bar graph showing proportion of fluorescent cells labelled using split GAL4 transgenics indicated and G-TRACE for *serpent* control and indicated VT lines (split GAL4 system). Red bars/dots show proportion of fluorescent cells in which only Red Stinger can be detected (current expression of split GAL4); yellow bars/dots show proportion of fluorescent cells in which both Red Stinger and Stinger can be detected (historical and current expression of split GAL4); green bars/dots show proportion of fluorescent cells in which only Stinger can be detected (historical expression of split GAL4, which has now ceased). Each point represents a dissected larva (n = 10, 7, 9, 10 and 9, from left to right for indicated genotypes). Bars and error bars show mean and standard deviation, respectively; bars annotated to show average number of cells counted across each category for 9 field of views. See ***Supplementary file 1*** for full list of genotypes.

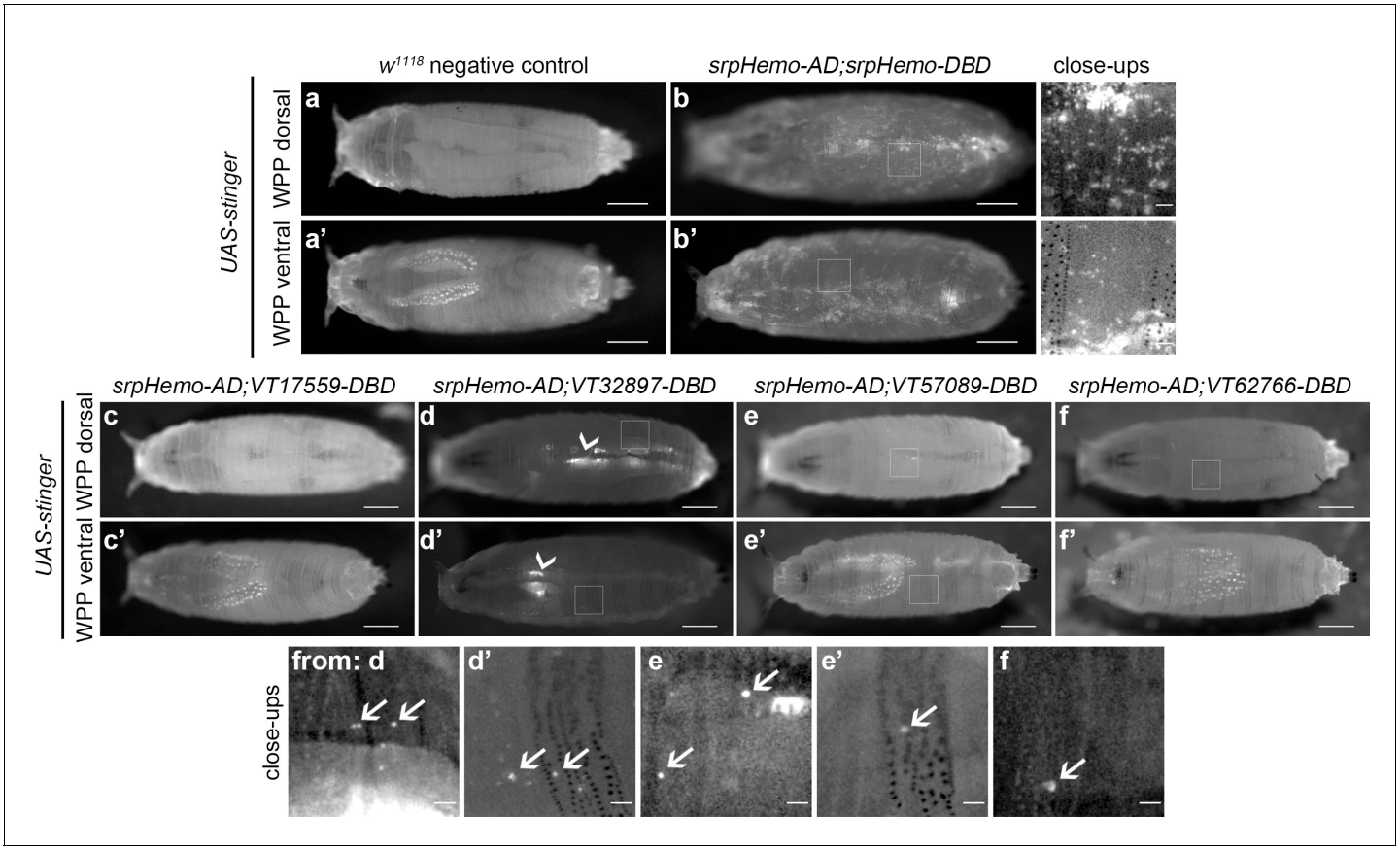

Figure 5. Plasmatocyte subpopulations are sparse in white pre-pupae. (**a–b**) Dorsal and ventral views of negative control (**a**, *UAS-stinger*, but no driver) and positive control (**b**, *UAS-stinger* driven by *srpHemo-AD;srpHemo-DBD*) white pre-pupae (WPP); boxes indicate regions shown in close-up views of positive controls. (**c–f**) dorsal and ventral views of WPP containing cells labelled using *srpHemo-AD* and the indicated *VT-DBD* to drive expression from *UAS-stinger*. Very few VT enhancer-labelled cells can be detected in WPP: boxes mark regions shown in close-up views with example hemocytes indicated with an arrow; dorsal vessel-associated and proventricular region/Garland cells can also be observed in *VT32897* WPP (arrowheads in **d** and **d'**, respectively); scale bars represent 500 µm (WPP) or 50 µm (close-ups); WPP images contrast enhanced to 0.3% saturation; close-up images contrast enhanced individually. See ***Supplementary file 1*** for full list of genotypes.

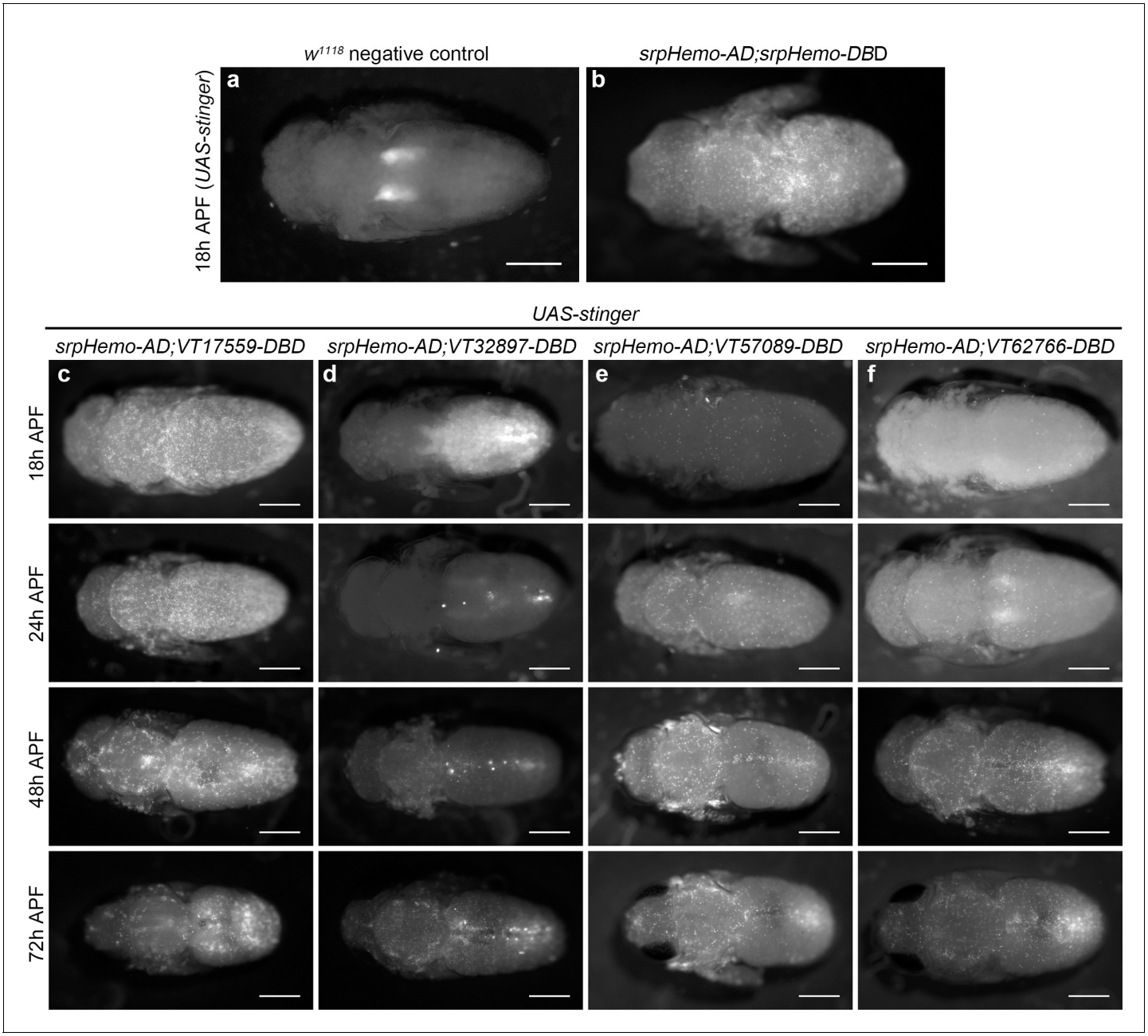

Figure 6. Plasmatocyte subpopulations return with distinct dynamics during pupal development. (**a–b**) Dorsal images of negative control (**a**, no GAL4) and positive control pupae (**b**, labelled via *srpHemo-AD;srpHemo-DBD*) at 18 hr after puparium formation (APF). (**c–f**) dorsal images showing localisation of cells labelled using *srpHemo-AD* and *VT-DBD* (VT enhancers used to drive *DBD* expression indicated above panels) to drive expression of *UAS-stinger* during pupal development from 18 hr AFP to 72 hr APF. All image panels contrast enhanced to 0.3% saturation to reveal localisation of labelled cells due to differing intensities of reporter line expression. Scale bars represent 500 μm. See ***Supplementary file 1*** for full list of genotypes.

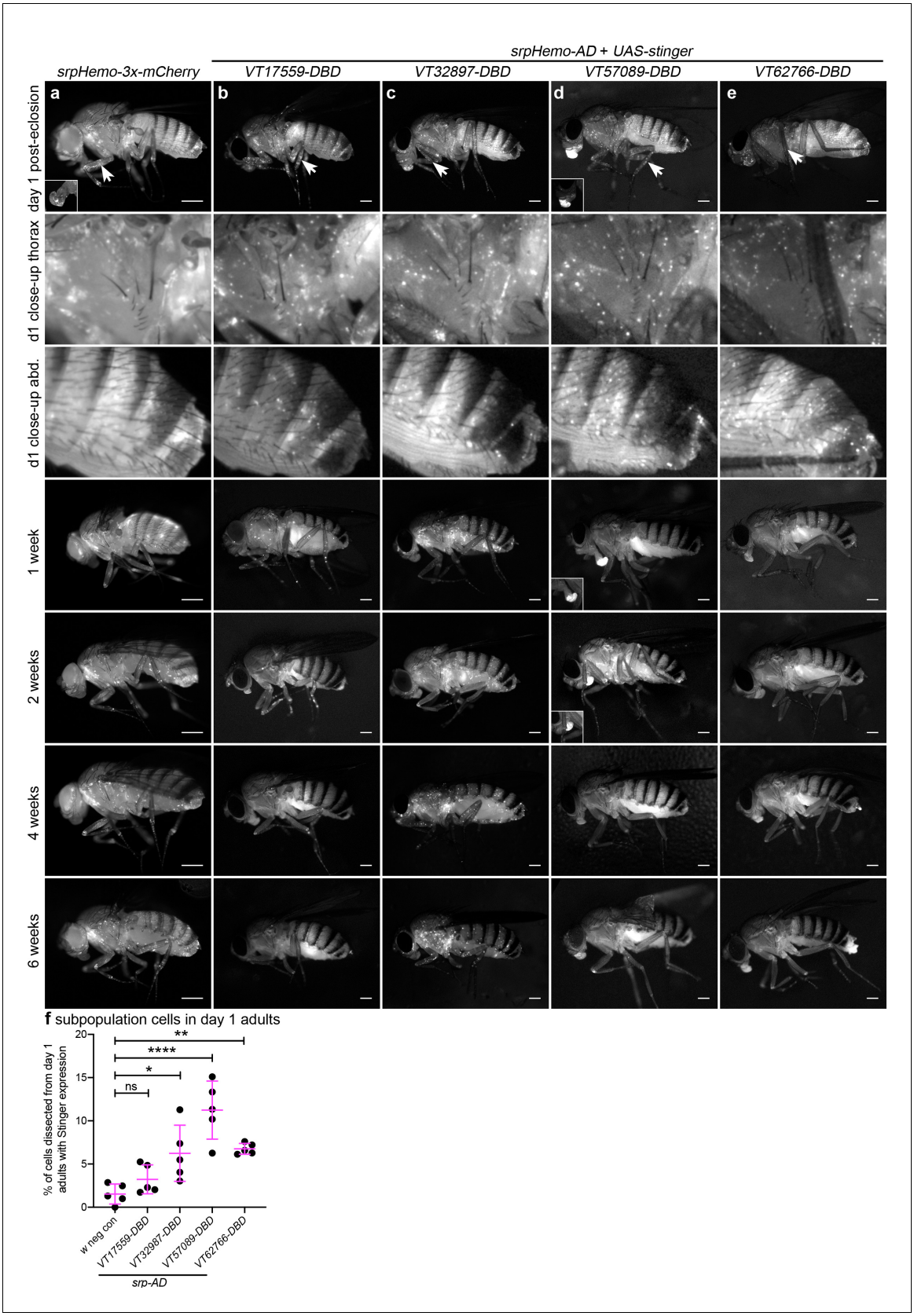

Figure 7. Plasmatocyte subpopulations exhibit distinct localisations and dynamics as adults age. (**a–e**) Representative lateral images of adult flies between 0 and 6 weeks of age showing localisation of cells labelled using *srpHemo-3x-mCherry* (**a**, positive control), or split GAL4 to drive expression

Figure 7 continued on next page

Figure 7 continued

of stinger (**b-e**, *srpHemo-AD;VT-DBD*). The VT enhancers used to drive expression of the DNA-binding domain (*DBD*) of *GAL4* correspond to *VT17559* (**b**), *VT32897* (**c**), *VT57089* (**d**), and *VT62766* (**e**); inset images show alternative view of proboscis region from same fly (**a**) or at a reduced level of brightness to reveal cellular detail (**d**). Images contrast enhanced to 0.15% saturation (**a–c, e**) or 0.75% (**d**) to reveal localisation of labelled cells due to differing intensities of reporter line expression. Arrows in top row indicate hemocytes in the legs; 2nd and 3rd rows show close-up of thorax and abdomen of day one flies; at least five flies were imaged for each timepoint; scale bars represent 500 μm. (**f**) Scatterplot showing proportion of cells dissected from day one adults that were labelled using *srpHemo-AD* and the *VT-DBD* transgenes indicated to drive expression from *UAS-stinger*. One-way ANOVA used to compare to negative control flies (w^{1118};*UAS-stinger/+*) with split GAL4 VT lines: n = 5 dissections per genotype; p=0.60 (*VT17559*), p=0.013 (*VT32897*), p<0.0001 (*VT57089*), and p=0.0063 (*VT62766*). Lines and error bars represent mean and standard deviation, respectively; ns, *, ** and **** denote not significant (p>0.05), p<0.05, p<0.01, and p<0.0001, respectively. See ***Supplementary file 1*** for full list of genotypes.

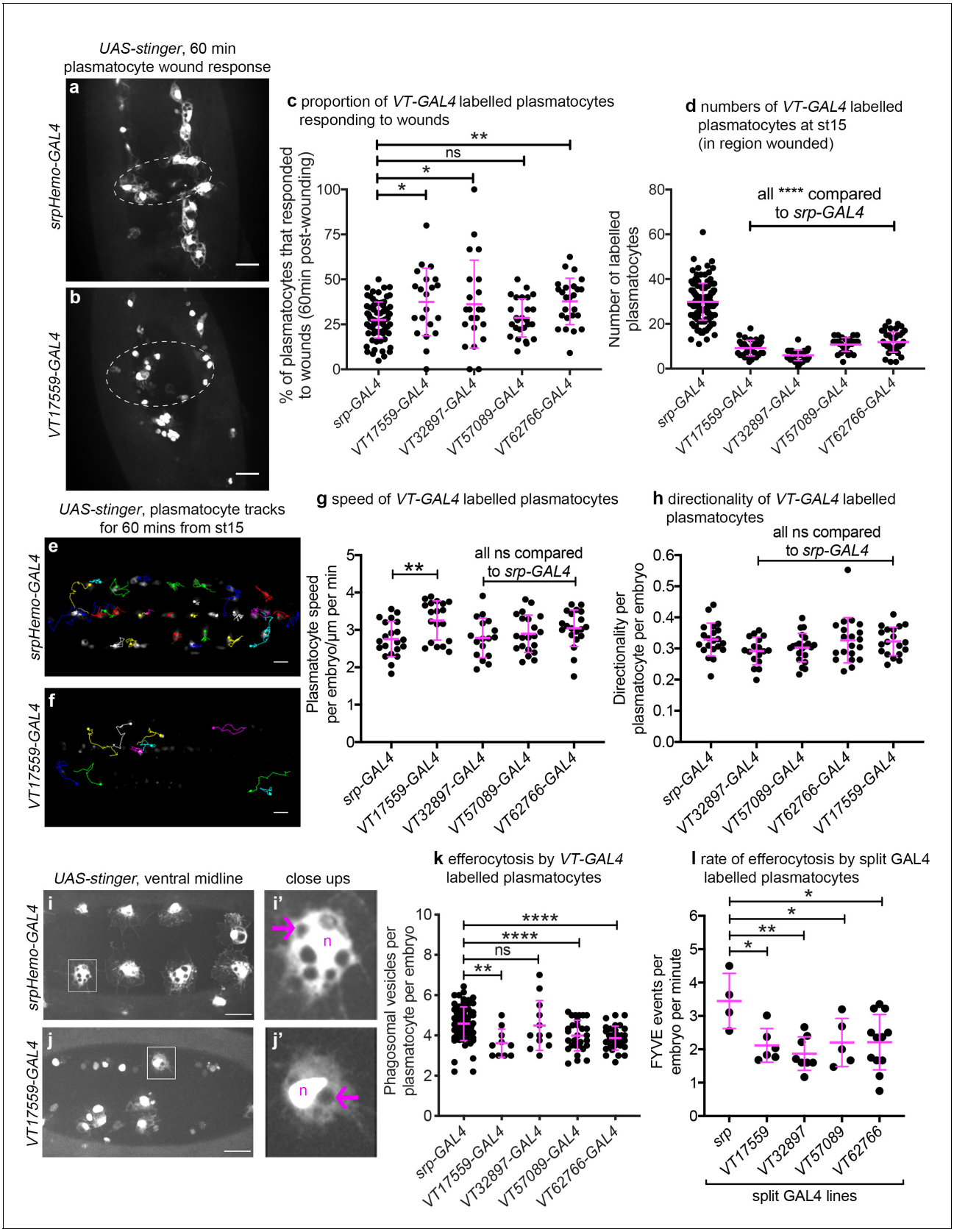

Figure 8. *Drosophila* plasmatocyte subpopulations demonstrate functional differences compared to the overall plasmatocyte population. (**a–b**) Example images showing plasmatocyte wound responses at 60 min post-wounding (maximum projections of 15 µm deep regions). Cells labelled via

Figure 8 continued on next page

Figure 8 continued

UAS-stinger using *srpHemo-GAL4* (**a**) and *VT17559-GAL4* (**b**); dotted lines show wound edges. (**c–d**) Scatterplots showing percentage of *srpHemo-GAL4* (control) or *VT-GAL4*-labelled plasmatocytes responding to wounds at 60 min (**c**) or total numbers of labelled plasmatocytes in wounded region (**d**); p=0.018, 0.041, 0.99, 0.0075 compared to *srpHemo-GAL4* (n = 77, 21, 22, 26, 25) (**c**); p<0.0001 compared to *srpHemo-GAL4* for all lines (n = 139, 35, 37, 30, 44) (**d**). (**e–f**) Example tracks of plasmatocytes labelled with GFP via *srpHemo-GAL4* (**e**) and *VT17559-GAL4* (**f**) during random migration on the ventral side of the embryo for 1 hr at stage 15. (**g–h**) Scatterplots showing speed per plasmatocyte, per embryo (**g**) and directionality (**h**) at stage 15 in embryos containing cells labelled via *srpHemo-GAL4* (control) or the *VT-GAL4* lines indicated; p=0.0097, 0.999, 0.82, 0.226 compared to *srpHemo-GAL4* (n = 21, 19, 17, 21, 20) (**g**); p=0.998, 0.216, 0.480, 0.999 compared to *srpHemo-GAL4* (n = 21, 19, 17, 21, 20) (**h**). (**i–j**) Example images of cells on the ventral midline at stage 15 with labelling via *UAS-stinger* expression using *srpHemo-GAL4* (**i**) and *VT17559-GAL4* (**j**); plasmatocytes shown in close-up images (**i', j'**) are indicated by white boxes in main panels; arrows show phagosomal vesicles, 'n' marks nucleus; n.b. panels contrast enhanced independently to show plasmatocyte morphology. (**k**) Scatterplot showing phagosomal vesicles per plasmatocyte, per embryo at stage 15 (measure of efferocytosis/apoptotic cell clearance); cells labelled via *srpHemo-GAL4* (control) or the *VT-GAL4* lines indicated; p=0.0020, 0.99, 0.0040, 0.0002 compared to *srpHemo-GAL4* (n = 76, 10, 12, 29, 31). (**l**) Scatterplot showing number of times 2x-FYVE-EGFP sensor recruited to phagosomes (FYVE events) per plasmatocyte, per embryo in plasmatocytes labelled via the split GAL4 system; p=0.019, 0.0034, 0.039 and 0.015 compared to *srp* control (n = 4, 6, 8, 5 and 12 embryos). Lines and error bars represent mean and standard deviation, respectively (all scatterplots); one-way ANOVA with a Dunnett's multiple comparison test used to compare VT lines with *srp* controls in all datasets; ns, *, **, and **** denote not significant (p>0.05), p<0.05, p<0.01, and p<0.0001, respectively. All scale bars represent 20 μm. See ***Supplementary file 1*** for full list of genotypes. N.b. ***Figure 8—figure supplements 1–3*** show analysis of subpopulation cell morphology, ROS levels and phagocytosis in response to immune challenge, respectively.

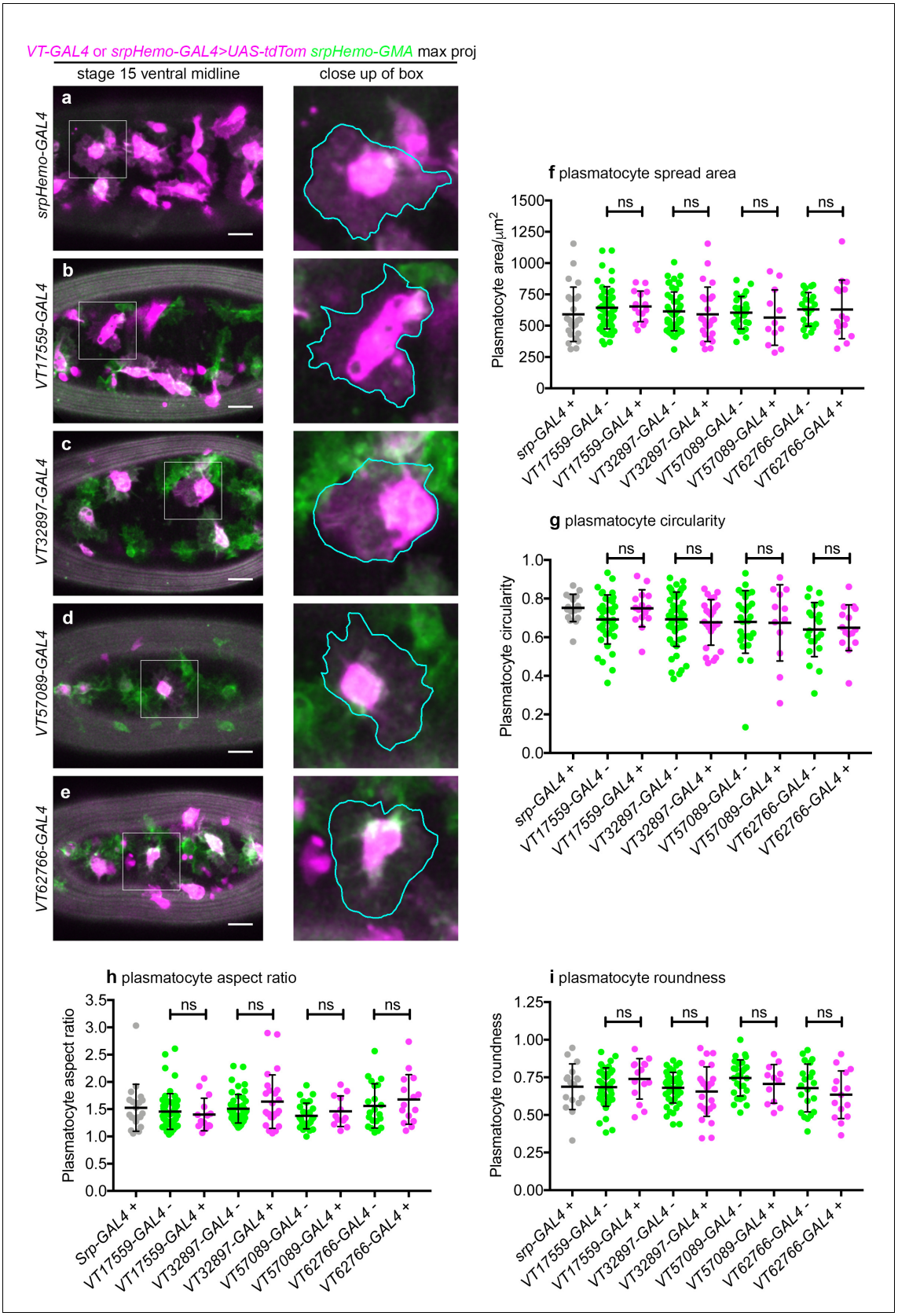

Figure 8—figure supplement 1. *VT-GAL4*-labelled subpopulations show no gross differences in morphology compared to non-labelled plasmatocytes. (**a–e**) Representative images of plasmatocytes at stage 15 on the ventral midline labelled using the pan-hemocyte marker *srpHemo-GMA* (green) and

Figure 8—figure supplement 1 continued on next page

Figure 8—figure supplement 1 continued

UAS-tdTomato (magenta) via *srpHemo-GAL4* (**a**), *VT17559-GAL4* (**b**), *VT32897-GAL4* (**c**), *VT57089-GAL4* (**d**), and *VT62766-GAL4* (**e**); scale bars represent 20 μm. Scatterplots showing plasmatocyte spread area (**f**), circularity (**g**), aspect ratio (**h**), and roundness (**i**) for positive control cells (labelled via *srpHemo-GAL4*), and *VT-GAL4*-positive/negative cells within embryos corresponding to those shown in (**a–e**). Cells positive for *VT-GAL4*-driven tdTomato expression were compared to non-tdTomato expressing cells via Student's t-test. No significant difference (ns) was found for any *VT-GAL4* line tested; lines and error bars represent mean and standard deviation, respectively; data points represent individual plasmatocytes taken from a minimum of three embryos. See ***Supplementary file 1*** for full list of genotypes.

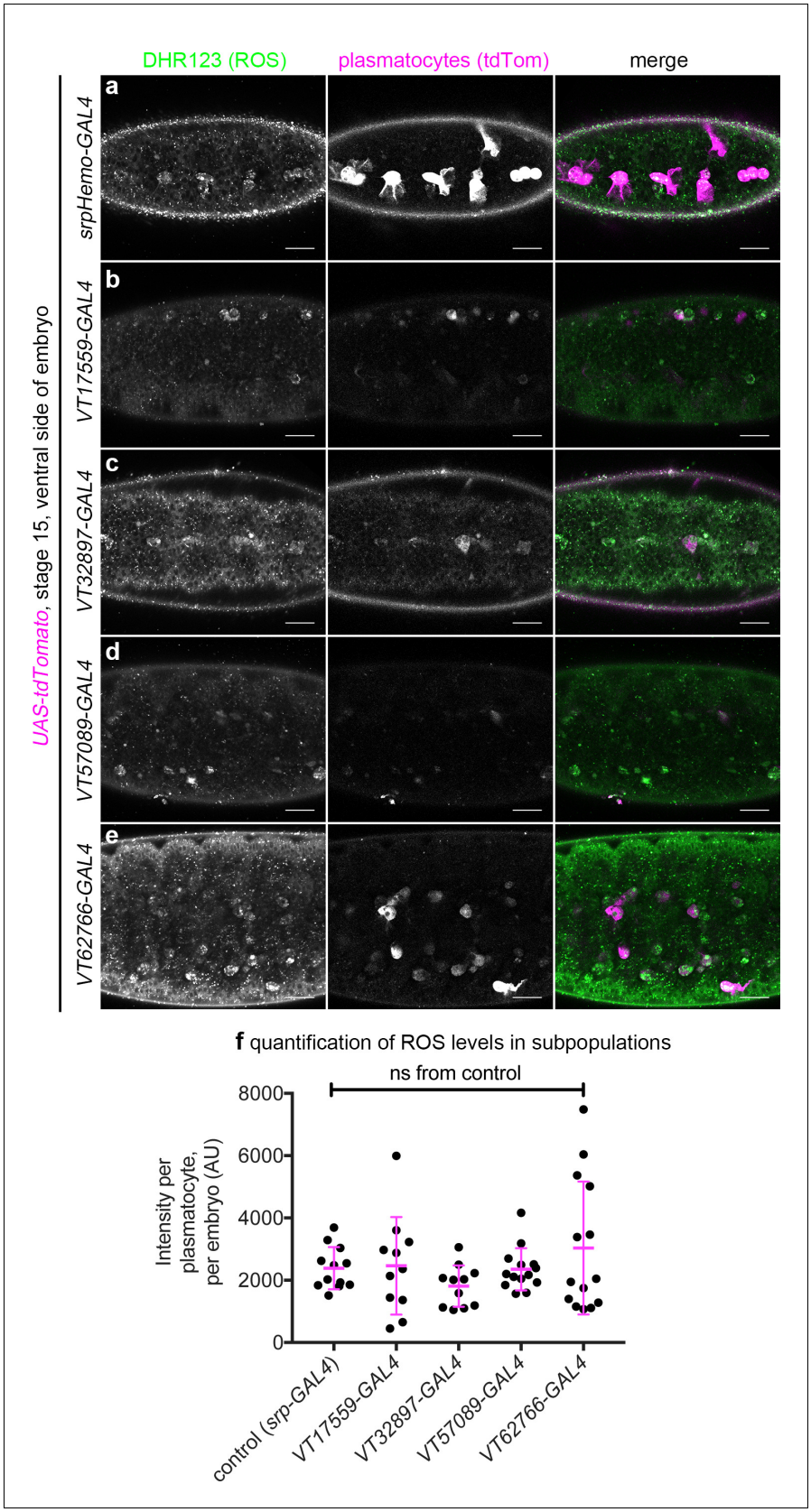

Figure 8—figure supplement 2. *VT-GAL4*-labelled plasmatocytes show no gross differences in their ROS levels compared to the overall population. (**a–e**) Representative images (single z-slices) of *VT-GAL4*-positive

Figure 8—figure supplement 2 continued on next page

Figure 8—figure supplement 2 continued

plasmatocytes (labelled via expression from *UAS-tdTomato*, magenta in merge) at stage 15 on the ventral midline stained via dihydrorhodamine 123 (DHR123) to show ROS levels (green in merge); *srpHemo-GAL4* was used as a positive control to show the overall population. (**f**) Scatterplot showing quantification of mean gray value per *srpHemo-GAL4* or *VT-GAL4*-labelled plasmatocyte, per embryo; lines and error bars represent mean and standard deviation, respectively. No statistically significant differences ($p>0.05$) were found between the *VT-GAL4* lines shown and the overall population (labelled via *srpHemo-GAL4*) using a one-way ANOVA compared to control; n = 12 (control); n = 11, $p>0.99$ (*VT17559-GAL4*); n = 11, $p=0.68$ (*VT32897-GAL4*); n = 14, $p>0.99$ (*VT57089-GAL4*); n = 14, $p=0.53$ (*VT62766-GAL4*) embryos; ns denotes not significantly different to control; scale bars represent 20 µm (**a–e**). See ***Supplementary file 1*** for full list of genotypes.

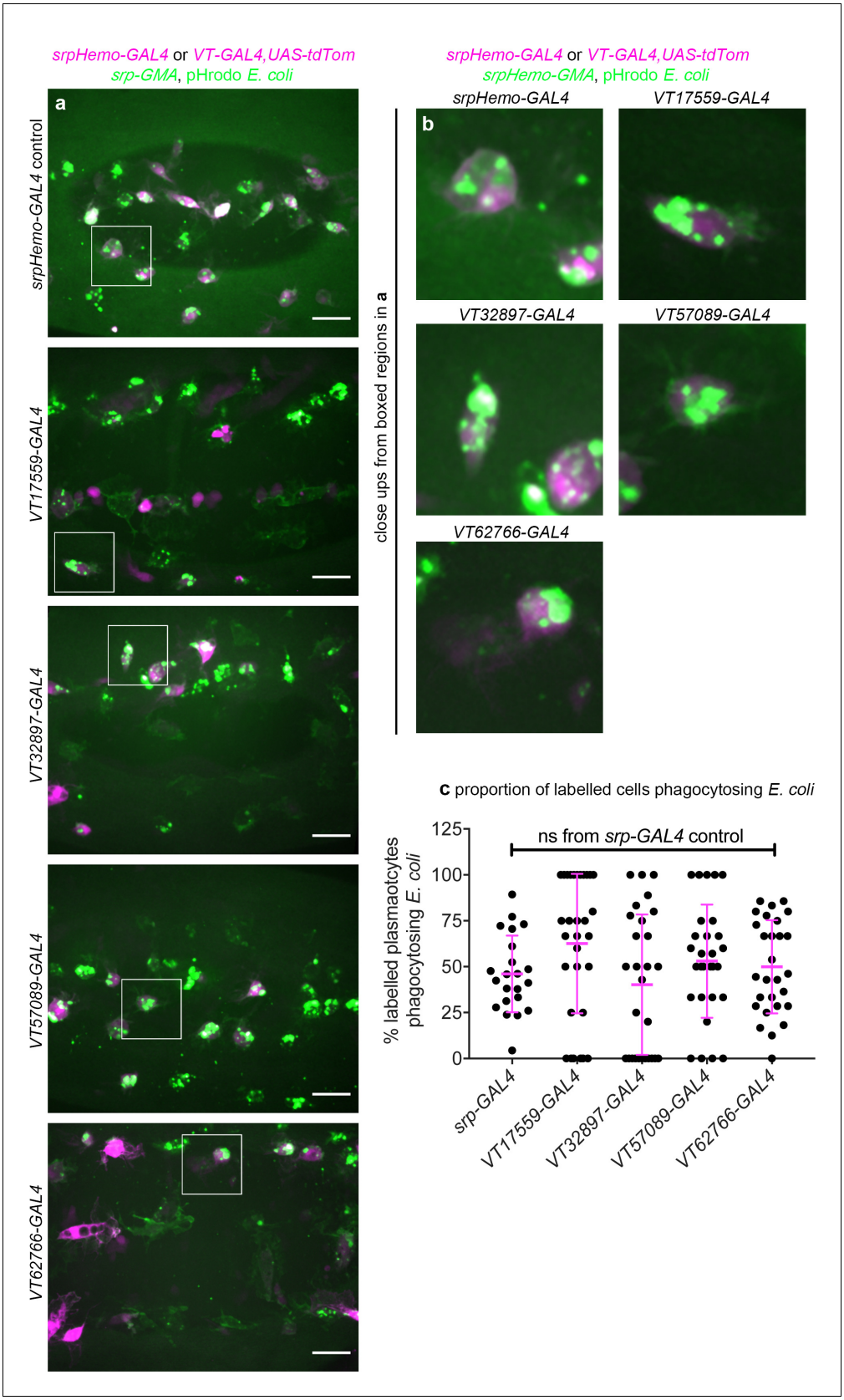

Figure 8—figure supplement 3. *VT-GAL4*-labelled plasmatocytes show no gross differences in their phagocytosis of *E. coli* compared to the overall population. (**a**) Ventral views of stage 15 embryos containing *srpHemo-GAL4* (positive control, overall population) and *VT-GAL4*-positive plasmatocytes

Figure 8—figure supplement 3 continued on next page

Figure 8—figure supplement 3 continued

(labelled via expression from *UAS-tdTomato*, magenta) 1 hr following injection with pHrodo-labelled *E. coli* particles (green); *srpHemo-GAL4* was used as a positive control to show the overall population; *srpHemo-GMA* used to label *VT-GAL4* negative plasmatocytes. (**b**) Shows close-ups of *E. coli*-positive plasmatocytes indicated by white boxes in (**a**). (**c**) Scatterplot showing quantification of the proportion of pHrodo *E. coli*-positive plasmatocytes per embryo in the populations labelled via *srpHemo-GAL4* or the indicated *VT-GAL4* reporter. Lines and error bars represent mean and standard deviation, respectively. No statistically significant difference (ns; p>0.05) was found between the *VT-GAL4* lines shown and plasmatocytes labelled via *srpHemo-GAL4* using a Kruskal-Wallis test with Dunn's multiple comparisons test: n = 22 (*srpHemo-GAL4*); n = 31, p=0.14 (*VT17559-GAL4*); n = 28, p>0.99 (*VT32897-GAL4*); n = 29, p>0.99 (*VT57089-GAL4*); n = 28, p>0.99 (*VT62766-GAL4*). Scale bars represent 20 μm. See ***Supplementary file 1*** for full list of genotypes.

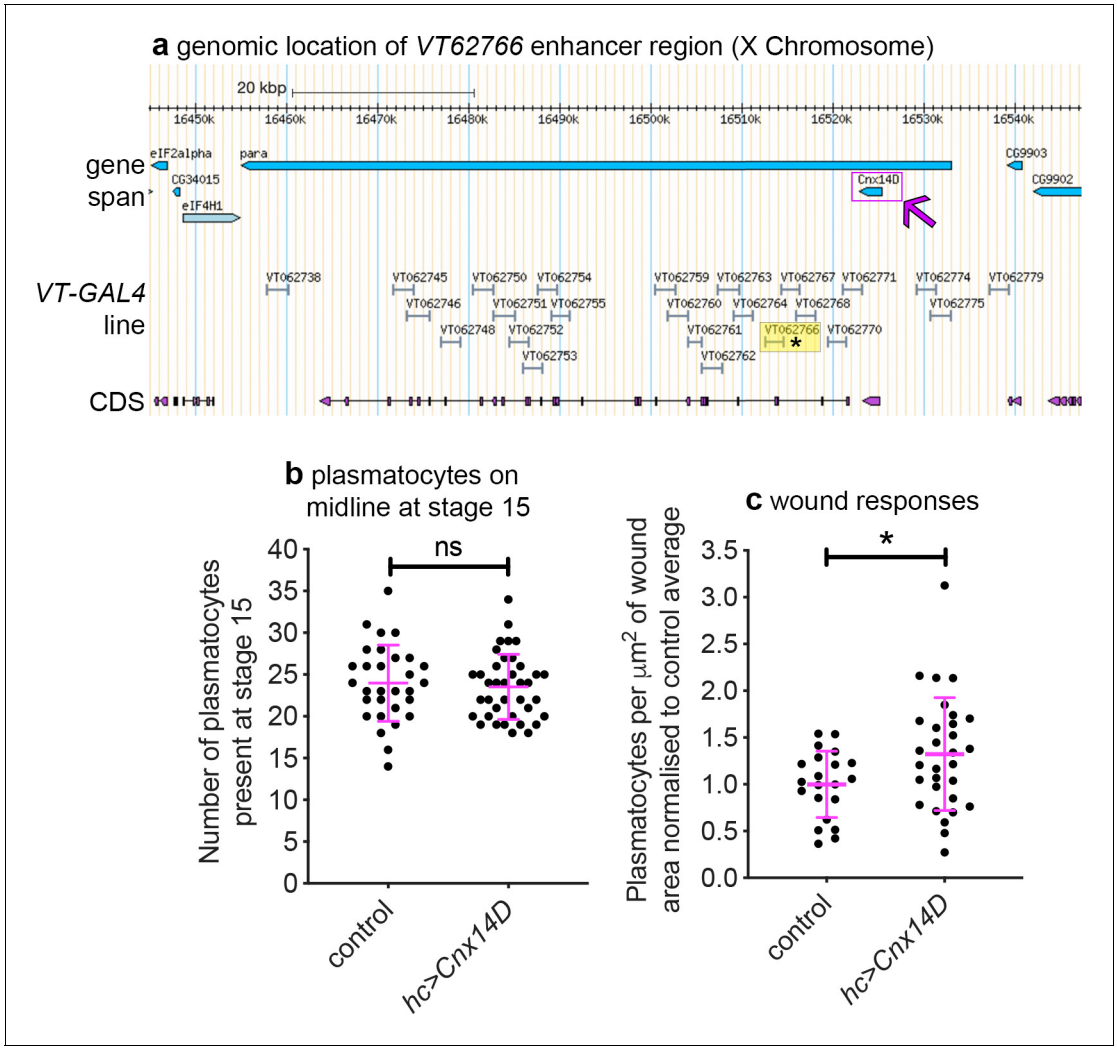

Figure 9. Misexpression of *Cnx14D* improves plasmatocyte inflammatory responses to injury. (**a**) Chromosomal location of the *VT62766-GAL4* enhancer region; only one transcript is shown for *para*, which possesses multiple splice variants. The *VT62766* region is highlighted in yellow and by an asterisk; *Cnx14D* (indicated by magenta arrow) lies within *para*. (**b**) Scatterplot showing numbers of plasmatocytes present at stage 15 on the ventral side of the embryo ahead of wounding in controls and on misexpression of *Cnx14D* in all hemocytes using both *srpHemo-GAL4* and *crq-GAL4* (*hc>Cnx14D*); n = 30 and 38 for control and *hc>Cnx14D* embryos, respectively, p=0.670 via Student's t-test. (**c**) Scatterplot of wound responses 60 min post-wounding (number of plasmatocytes at wound, normalised for wound area and to control responses); n = 21 and 30 for control and *hc>Cnx14D* embryos, respectively; p=0.0328 via Student's t-test. Line and error bars represent mean and standard deviation, respectively (**b–c**). See ***Supplementary file 1*** for full list of genotypes.

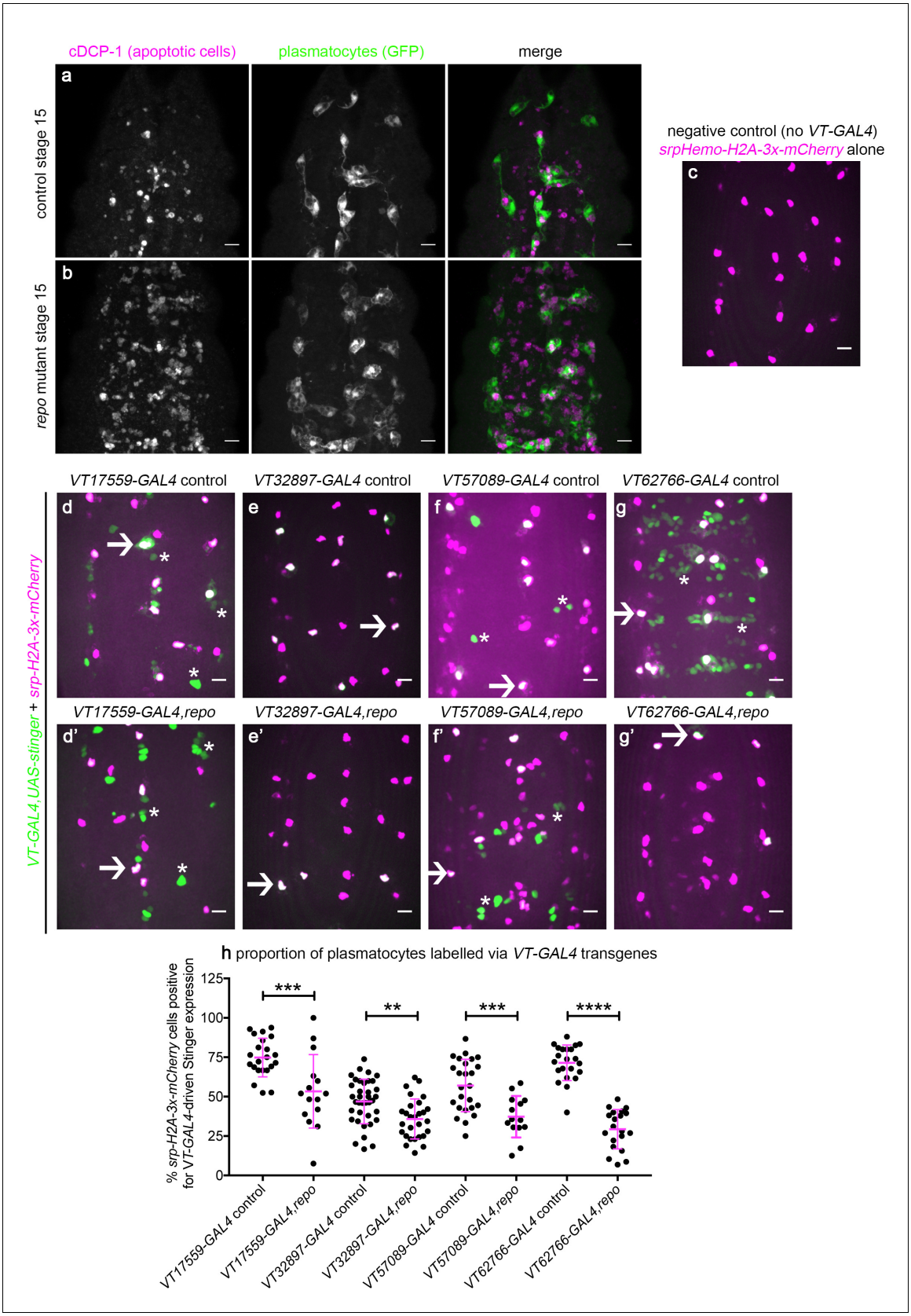

Figure 10. *Drosophila* plasmatocyte subpopulation identity can be controlled through exposure to apoptotic cells. (**a–b**) Maximum projections showing apoptotic cells (via anti-cDCP-1 staining, magenta in merge) and plasmatocytes (via anti-GFP staining, green in merge) at stage 15 on the ventral

Figure 10 continued on next page

Figure 10 continued

midline in control (**a**) and *repo* mutant embryos (**b**). (**c–g**) maximum projections of the ventral midline showing a negative control embryo (**c**) and embryos containing *VT-GAL4*-labelled plasmatocytes at stage 15 in control (**d–g**) and *repo* mutant embryos (**d'–g'**). *VT-GAL4* used to drive *UAS-stinger* expression (green) and *srpHemo-H2A-3x-mCherry* used to label plasmatocytes (magenta). Arrows and asterisks indicate examples of *VT-GAL4*-positive plasmatocytes and non-plasmatocyte cells, respectively; note loss of non-plasmatocyte *VT-GAL4* expression in *repo* mutants versus controls for *VT62766-GAL4*. (**h**) Scatterplot showing percentage of H2A-3x-mCherry-positive cells that are also positive for *VT-GAL4* driven Stinger expression in control and *repo* mutant embryos at stage 15. Student's t-test used to show significant difference between controls and *repo* mutants ($p=0.0009$, $n = 22, 15$ for *VT17559-GAL4* lines; $p=0.0017$, $n = 37, 28$ for *VT32897-GAL4* lines; $p=0.0005$, $n = 25, 14$ for *VT57089-GAL4* lines; $p<0.0001$, $n = 22, 20$ for *VT62766-GAL4* lines). Scale bars represent 10 μm (**a–g**); lines and error bars represent mean and standard deviation (**h**); **, ***, and **** denote $p<0.01$, $p<0.001$, and $p<0.0001$, respectively. See ***Supplementary file 1*** for full list of genotypes.